

**Suppressed Auger scattering and tunable light emission of Landau-quantized massless Kane electrons**

But, D. B.; Mittendorff, M.; Consejo, C.; Teppe, F.; Mikhailov, N. N.; Dvoretiskii, S. A.; Faugeras, C.; Winnerl, S.; Helm, M.; Knap, W.; Potemski, M.; Orlita, M.;

Originally published:

August 2019

**Nature Photonics 13(2019), 783-787**

DOI: <https://doi.org/10.1038/s41566-019-0496-1>

Perma-Link to Publication Repository of HZDR:

<https://www.hzdr.de/publications/Publ-29460>

Release of the secondary publication  
on the basis of the German Copyright Law § 38 Section 4.

# Suppressed Auger scattering and tunable light emission of Landau-quantized massless Kane electrons

D. B. But,<sup>1,2</sup> M. Mittendorff,<sup>3,4</sup> C. Consejo,<sup>1</sup> F. Teppe,<sup>1</sup> N. N. Mikhailov,<sup>5</sup> S. A. Dvoretiskii,<sup>5</sup>  
C. Faugeras,<sup>6</sup> S. Winnerl,<sup>3</sup> M. Helm,<sup>3</sup> W. Knap,<sup>1,2</sup> M. Potemski,<sup>6</sup> and M. Orlita<sup>6,7,\*</sup>

<sup>1</sup>Laboratoire Charles Coulomb, UMR CNRS 5221,  
University of Montpellier, Montpellier 34095, France

<sup>2</sup>International Research Centre CENTERA, Institute of High Pressure Physics,  
Polish Academy of Sciences, 01-142 Warsaw, Poland

<sup>3</sup>Helmholtz-Zentrum Dresden-Rossendorf, PO Box 510119, 01314 Dresden, Germany

<sup>4</sup>Universität Duisburg-Essen, Fakultät für Physik, 47057 Duisburg, Germany

<sup>5</sup>A.V. Rzhanov Institute of Semiconductor Physics, Siberian Branch,  
Russian Academy of Sciences, Novosibirsk 630090, Russia

<sup>6</sup>Laboratoire National des Champs Magnétiques Intenses,  
CNRS-UGA-UPS-INSA-EMFL, 25 rue des Martyrs, 38042 Grenoble, France

<sup>7</sup>Charles University, Faculty of Mathematics and Physics,  
Ke Karlovu 5, 121 16 Prague 2, Czech Republic

(Dated: April 25, 2019)

The Landau level laser has been proposed a long time ago as a unique source of monochromatic radiation, widely tunable in the THz and infrared spectral ranges using an externally applied magnetic field. In spite of decades of efforts, this appealing concept never resulted in the design of a reliable device. This is due to efficient Auger scattering of Landau-quantized electrons, which is an intrinsic non-radiative recombination channel that eventually gains over cyclotron emission in all materials studied so far: in conventional semiconductors with parabolic bands, but also in graphene with massless electrons. The Auger processes are favored in these systems by Landau levels (or their subsets) equally spaced in energy. Here we show that this scheme does not apply to massless Kane electrons in gapless HgCdTe alloy, in which undesirable Auger scattering is strongly suppressed and the sizeable cyclotron emission observed, for the first time in the case of massless particles. The gapless HgCdTe thus appears as a material of choice for future technology of Landau level lasers.

When a magnetic field is applied to a solid, the continuous density of electronic states transforms into a set of discrete energy levels, known as Landau levels (LLs). Electrons excited in such a ladder may recombine with emission of photons. This process can be viewed as an inverse of cyclotron resonance<sup>1</sup> and it is referred to as cyclotron emission<sup>2-5</sup>. The idea to construct the LL laser by achieving stimulated cyclotron emission<sup>2</sup> is as old as the experimental realization of the very first laser itself<sup>6</sup>. The tunability represents a great advantage of this concept. The strength of the magnetic field defines the spacing between LLs, and therefore, also the emission frequency of the laser. This frequency typically corresponds to the far infrared (terahertz) spectral range. The successful realization of the LL laser<sup>2,7-10</sup> would thus bridge

the so-called terahertz gap<sup>11,12</sup>, which still exists despite a considerable effort of several generations of physicists.

There is, however, a fundamental difficulty that has been recognized during the very first attempts to test the concept of a LL laser. In conventional materials, with quadratically dispersing electronic bands, and therefore, with equally spaced LLs,  $E_N^S = \hbar\omega_c(N + 1/2)$  for  $N = 0, 1, 2$ , cyclotron emission is an intrinsically weak process<sup>2,3,13</sup>. This is due to two independent processes which compete with cyclotron emission: reabsorption of cyclotron radiation<sup>2</sup> and Auger inter-LL recombination<sup>14,15</sup> (Fig. 1a). The latter becomes at higher pumping rates extremely efficient for electrons within the equidistant LL ladder, and in consequence, the excited LLs become depleted with a characteristic rate proportional to the number of electrons in this level ( $\tau^{-1} \propto n$ ). Stronger pumping, either optical or electrical, in systems with parabolic bands does not enhance cyclotron emission, but instead, increases the probability of Auger scattering. The inversion of population thus cannot be achieved. Electrons promoted via Auger processes to higher LLs then relax via non-radiative channels, most often by emission of optical phonons<sup>3</sup>.

To overcome this obstacle, various systems with non-equidistant LLs have been proposed as appropriate materials for a LL laser<sup>2,16</sup>. These may be found, for instance, in different narrow-gap materials or in the valence band of zinc-blende semiconductors. So far, stimulated cyclotron emission was achieved only in bulk germanium in which a non-equidistant spacing of valence-band LLs was created by crossed electric and magnetic fields<sup>17</sup>, alas in the regime close to the electrical breakdown of this material. In other attempts, quantum cascade structures have also been tested to achieve efficient cyclotron emission<sup>18,19</sup>.

Renewed impetus to investigate cyclotron emission came along with the fabrication of graphene, which was considered as an ideal system with non-equidistant LLs

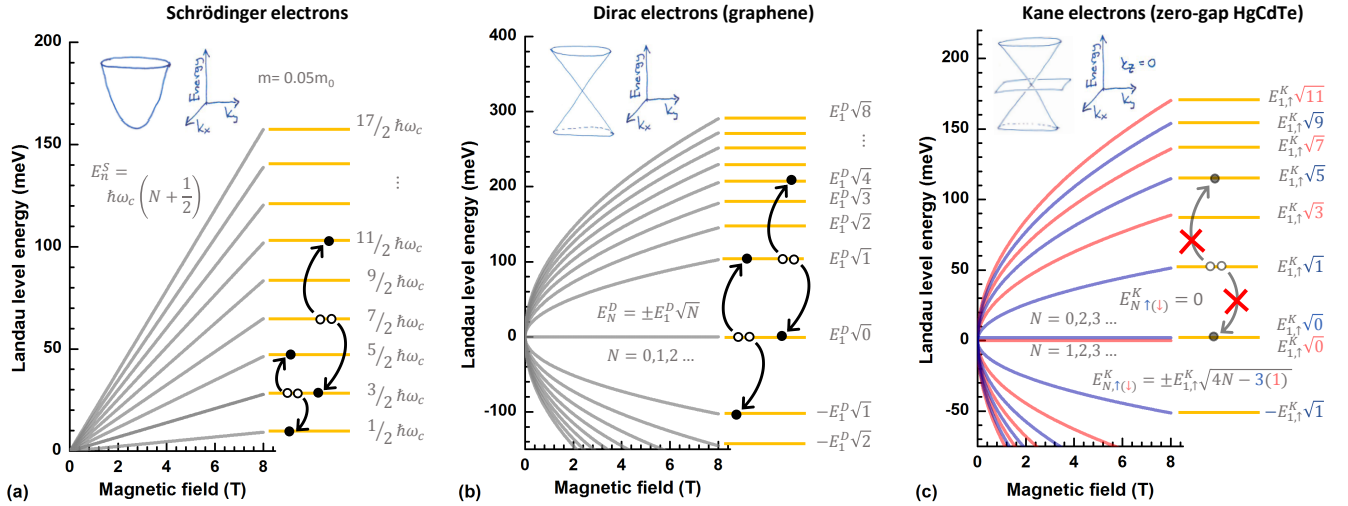


FIG. 1. Landau level ladders and possible paths for Auger scattering of massive and massless electrons. The  $B$ -dependence and spacing of Landau levels for conventional massive (Schrödinger) electrons, Dirac electrons in graphene and massless Kane electrons (at  $k = 0$ ), in part (a), (b) and (c), respectively. The arrows in LL ladders correspond to the Auger scattering processes discussed in the main text.

for the implementation of the LL laser<sup>10,20</sup>. Its conical band may be viewed as an extreme case of non-parabolicity and implies a specific sequence of Landau levels,  $E_N^D = \pm v\sqrt{2e\hbar BN}$  for  $N = 0, 1, 2, \dots$ , with the  $\sqrt{N}$  spacing, typical of massless Dirac electrons (Fig. 1b). However, to the best of our knowledge, no cyclotron emission, let alone the Landau level laser based on graphene, has been reported so far, despite pertinent theoretical predictions and numerous experimental attempts<sup>10,20–26</sup>.

This surprising lack of optical emission seems to be still a consequence of Auger scattering. Initially, such processes were expected to vanish in Landau-quantized graphene, but finally they were experimentally proven to be present and very efficient<sup>27,28</sup>. The reason behind is simple. The LL spectrum in graphene:  $E_N^D \propto \sqrt{N}$  for  $N = 0, 1, 2, \dots$ , includes subsets of equidistant levels. For instance, LLs with indices  $N = 0, \pm 1, \pm 4, \pm 9, \dots$  or  $0, \pm 2, \pm 8, \pm 18, \dots$ , are equally spaced and may thus support, similar to conventional materials, efficient Auger recombination (Fig. 1b). Notably, such a conclusion is valid not only for graphene, but for any other system with a conical band described by the Dirac Hamiltonian for particles with a zero rest mass.

Fortunately, one may find other systems with massless electrons, described by a Hamiltonian that differs from the Dirac one. In such systems, equidistantly spaced LLs may be avoided and undesirable Auger scattering possibly suppressed. In this paper, we test Landau-quantized 3D massless Kane electrons<sup>29–32</sup> against the efficiency of Auger scattering and against the possibility of efficient LL emission. This type of massless electrons appears in conventional bulk zinc-blende semiconductors when their energy band gap – the parameter responsible for the gen-

eration of the non-zero band mass of electrons and holes, and therefore, also Schrödinger-like behavior of these carriers – vanishes, for instance, in the ternary compound HgCdTe explored in this paper.

In magnetic fields, the conical band of 3D massless Kane electrons splits into LLs, or more precisely, Landau bands, which resemble those of massless Dirac electrons<sup>33</sup>:

$$E_{N,\sigma}^K(k) = \pm v\sqrt{2e\hbar B(N - 1/2 + \sigma/2) + \hbar^2 k^2}, \quad (1)$$

where  $N = 1, 2, 3, \dots$  is the LL index,  $k$  the momentum along the applied magnetic field and  $v$  the velocity parameter. However, the splitting due to spin is given by  $\sigma = \pm 1/2$  and differs from the one known for genuine Dirac-type electrons ( $\sigma = \pm 1$ ). As a result, the LL spectrum of massless Kane electrons (Fig. 1c):  $E_N^K \propto \sqrt{N}$  for  $N = 0, 1, 3, 5, \dots$ , does not include any subsets of equally spaced LLs at  $k = 0$ , where the maxima in the density of states are. In contrast, 3D Dirac electrons with  $\sigma = \pm 1$  display at  $k = 0$  the spacing  $E_N^D \propto \sqrt{N}$  where  $N = 0, 1, 2, 3, \dots$ , which is identical to that of 2D graphene.

Moreover, there exists a set of narrowly spaced LLs, which originates from the weakly dispersing (nearly flat) band. In the simplest approach, these LLs do not disperse with  $B$ :  $E_{n,\sigma}^K = 0$  for  $n = 0, 2, 3, 4, \dots$ . Excitations from this flat band to conduction-band LLs constitute a dominant contribution to the optical response at low photon energies and follow the standard selection rules,  $N \rightarrow N \pm 1$ , for electric-dipole transitions<sup>31,32,34</sup>.

To test Landau-quantized electrons in gapless HgCdTe for the presence of Auger scattering, we have employed a degenerate pump-probe technique, using the free-electron

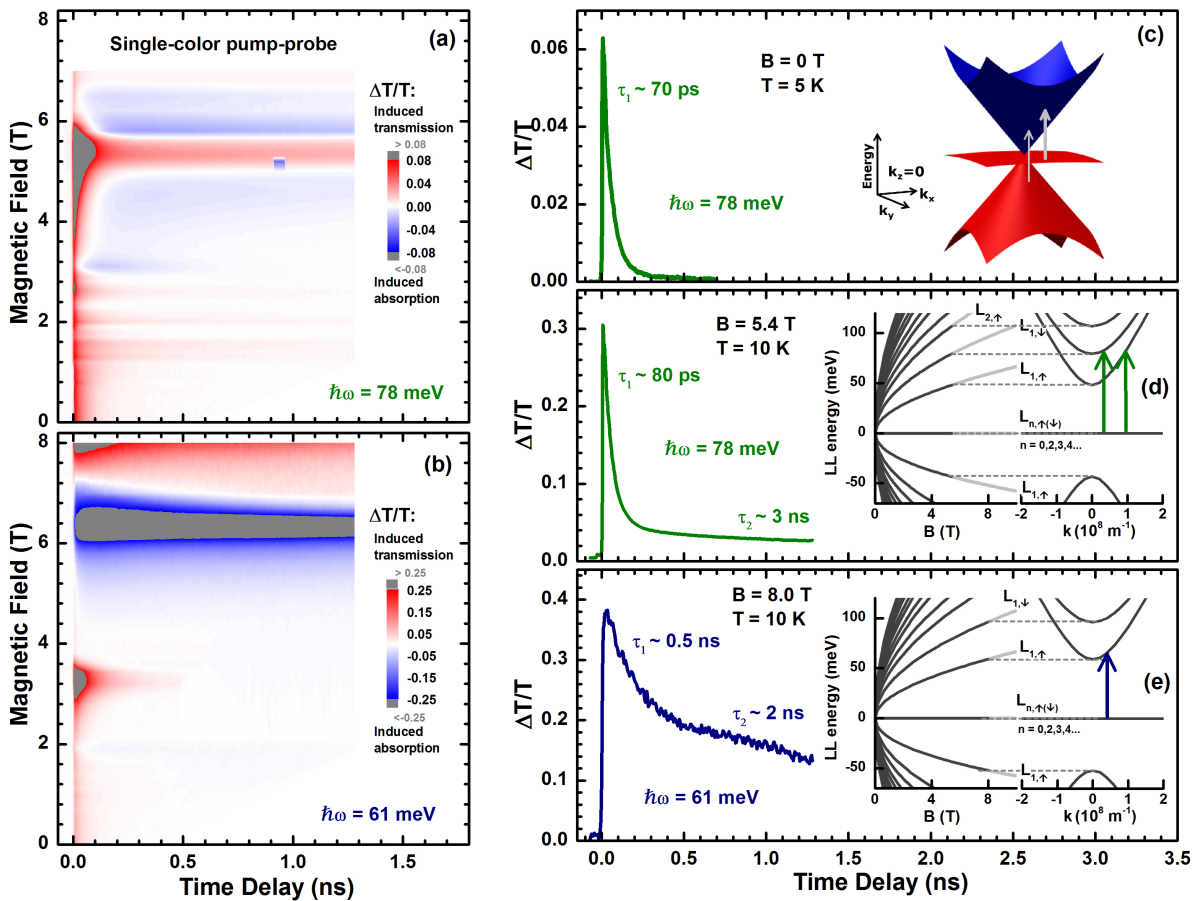


FIG. 2. **Pump-probe experiments and Auger scattering of Landau-quantized massless Kane electrons.** (a) and (b) False-color maps of induced transmission  $\Delta T/T$  measured at  $T = 10$  K and for laser photon energies  $\hbar\omega = 78$  meV (upper panel) and 61 meV (lower panel) as a function of the time delay and magnetic field, showing both, pronounced induced transmission ( $\Delta T/T > 0$ ) and absorption ( $\Delta T/T < 0$ ). (c-e) Selected pump-probe transients. The inter-LL excitations in (d) and (e) follow the standard selection rules for electric-dipole transitions which are active in linearly polarized light,  $N \rightarrow N \pm 1$ , and schematically shown in the corresponding insets.

laser emitting  $\sim 3$ -ps-long pulses in the mid-infrared range. The results are plotted in Figs. 2a and b, in the form of false color-maps, for two different photon energies of the laser. These maps show pump-probe transients, *i.e.*, the pump-induced relative change of transmission,  $\Delta T/T$ , as a function of the applied magnetic field and time delay between pump and probe pulses. One immediately concludes that  $\Delta T/T$  undergoes a fairly complex evolution in both, its amplitude and sign, on a characteristic time scale extending up to nanoseconds.

To illustrate the observed behavior in greater detail, three selected pump-probe traces are plotted in Figs. 2c-e. At  $B = 0$ , the observed induced transmission (bleaching) is primarily due to electrons excited from the fully occupied heavy-hole-like flat band to the upper conical band (inset of Fig. 2c). The contribution of excitations from the lower cone is considerably weaker. The induced transmission exhibits a nearly mono-exponential decay, with a characteristic time,  $\tau = 70$  ps, which is comparable to that in other gapless systems with conical bands,

such as graphene<sup>35</sup>. This relatively fast relaxation may be associated with the emission of phonons.

When the magnetic field is applied, one observes a pronounced change in  $\Delta T/T$  transients. For particular values of  $B$ , the second component develops, with a characteristic decay time in the nanosecond range. The appearance of this slow component clearly coincides with the resonant pumping into the bottom of Landau bands. This is illustrated in Fig. 2d, where the  $\Delta T/T$  trace collected at  $B = 5.4$  T and  $\hbar\omega = 78$  meV is plotted. In this particular case, electrons are pumped from the flat band to two lowest lying conduction-band LLs, see the inset of Fig. 2d. The faster component, with a relaxation rate not much different from the zero-field one ( $\tau \approx 80$  ps), can be associated with the relaxation of electrons excited into the lowest Landau band ( $E_{1,\uparrow}^K$ ). **This relaxation of electrons from states with finite-momentum towards  $k \approx 0$  is probably due to emission of phonons.** Most likely, electrons relax via emission of acoustic phonons. The slow component, appearing only when electrons are

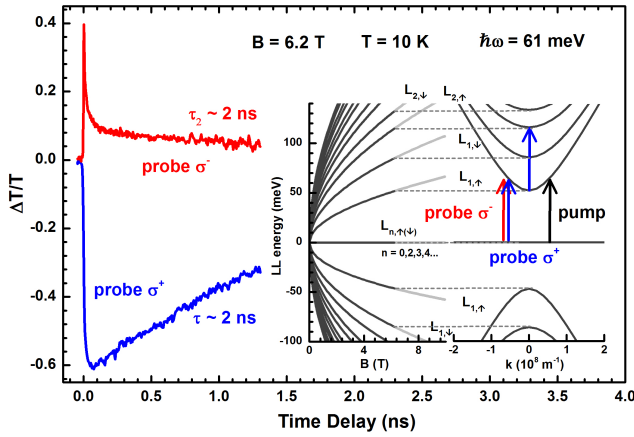


FIG. 3. **Pump-probe experiments using circularly polarized probe beam.** Pump-probe transients collected at  $B = 6.2$  T using the laser photon energy of  $\hbar\omega = 61$  meV and circularly polarized probe beam. The involved excitations, which follow the standard electric-dipole selection rules for right and left circularly polarized radiation:  $N \rightarrow N + 1$  and  $N \rightarrow N - 1$ , respectively, are schematically shown in the inset.

198 pumped resonantly from/to states around  $k \approx 0$ , reflects  
 199 the existence of long-living electrons at the bottom of the  
 200  $E_{1,\downarrow}^K$  Landau band. Another example of the slowly decay-  
 201 ing component in the pump-probe transient is shown in  
 202 Fig. 2e. This  $\Delta T/T$  trace was collected at  $B = 8$  T and  
 203  $\hbar\omega = 61$  meV, when only the lowest LL in the conduction  
 204 band ( $E_{1,\uparrow}^K$ ) is pumped close to zero-momentum states.

205 Experiments with circularly polarized radiation repre-  
 206 sent another way to visualize how the relaxation of photo-  
 207 excited electrons in gapless HgCdTe is slowed-down when  
 208 the magnetic field is applied. Pump-probe transients col-  
 209 lected using a linearly polarized pump pulse, but with a  
 210 circularly polarized probe pulse are depicted in Fig. 3.  
 211 In this particular case, electrons are excited by the pump  
 212 pulse from the flat band to the lowest lying LL only,  
 213 as schematically shown by the vertical arrow in the in-  
 214 set of Fig. 3. The transient recorded using  $\sigma^-$ -polarized  
 215 probe shows positive  $\Delta T/T$ , with an initial fast decay  
 216 due to the relaxation of electrons to the bottom of  $E_{1,\uparrow}^K$   
 217 level and slower component indicating a nanosecond-long  
 218 lifetime of excited electrons around  $k \approx 0$ . Different be-  
 219 havior, *i.e.*, strong induced absorption  $\Delta T/T < 0$ , is  
 220 observed when the probing beam is  $\sigma^+$  polarized. In this  
 221 latter case, the induced absorption is primarily due to the  
 222  $E_{1,\uparrow}^K \rightarrow E_{2,\uparrow}^K$  transition which becomes activated due to  
 223 electrons promoted to the  $E_{1,\uparrow}^K$  level by the pump pulse.  
 224 This excitation corresponds to the fundamental cyclotron  
 225 mode, which becomes resonant with the laser photon en-  
 226 ergy ( $\hbar\omega = 61$  meV) just at the selected magnetic field  
 227 of  $B = 6.2$  T.

228 Let us now discuss the main findings of our pump-  
 229 probe experiments. These show that electrons in Landau-  
 230 quantized gapless HgCdTe relax with relatively long de-  
 231 cay times, at the scale of nanoseconds. In addition, the  
 232 presented pump-probe experiments were performed at

233 relatively high photon fluences,  $\sim 0.5 \mu\text{J}\cdot\text{cm}^{-2}$ . These  
 234 translate, for the chosen photon energy, into the photon  
 235 flux of  $10^{14} \text{ cm}^{-2}$  per pulse. Due to the relatively large  
 236 absorption coefficient<sup>31</sup>, which in the linear regime, at  
 237  $\hbar\omega \approx 70$  meV and  $B = 0$ , reaches  $\lambda \approx 3 \times 10^3 \text{ cm}^{-1}$ , a  
 238 significant part of the flux is absorbed in the explored 3-  
 239  $\mu\text{m}$ -thick layer of gapless HgCdTe. This corresponds to  
 240 more than  $10^{16} \text{ cm}^{-3}$  electrons promoted from the flat  
 241 band to the upper conical band by a single pump pulse.  
 242 Since there is no decay observed at the scale of the pulse  
 243 duration ( $\sim 3$  ps), this number serves as a rough estimate  
 244 of the electron density in the sample just after the pump  
 245 pulse.

246 One may compare this carrier density and the deduced  
 247 relaxation time, with the results obtained in conven-  
 248 tional semiconductors, where a strong decrease of relax-  
 249 ation time with the electron density has been reported:  
 250  $\tau \propto n^{-1}$ , see Refs. 3, 13, and 36. In conventional semi-  
 251 conductors, the nanosecond decay times are only found  
 252 at very low carrier densities in the excited LL, in the  
 253 range of  $10^{12}$ - $10^{13} \text{ cm}^{-3}$ . For the carrier density close  
 254 to  $10^{16} \text{ cm}^{-3}$  in a parabolic-band semiconductor, one ex-  
 255 pects the electron relaxation time to drop down to the  
 256 sub-picosecond range<sup>3</sup> due to efficient Auger processes.  
 257 This is more than three orders of magnitude less than  
 258 relaxation times observed in gapless HgCdTe in a mag-  
 259 netic field. This indicates that Auger scattering is indeed  
 260 strongly suppressed for Landau-quantized massless Kane  
 261 electrons as compared to other materials explored so far.  
 262 We interpret this suppression as a direct consequence of  
 263 the specific LL spectrum, which does not include any  
 264 subset of equidistant levels (around  $k \approx 0$ ).

265 Since the rate inter-LL Auger scattering follows the de-  
 266 generacy of Landau levels ( $\propto B$ ) and the strength of in-  
 267 teraction between Landau-quantized electrons ( $\propto \sqrt{B}$ )<sup>37</sup>,  
 268 we expect similarly long lifetimes also at lower magnetic  
 269 fields. Let us also note that the observed lifetime of  
 270 electrons, even though unusually long as compared to  
 271 any so-far explored Landau-quantized semiconductor or  
 272 semimetal<sup>3</sup>, remains still significantly shorter than spon-  
 273 taneous cyclotron radiative lifetime. This latter time  
 274 can be for massless electrons estimated using the simple  
 275 formula<sup>10</sup>,  $\tau_{\text{sp}}^{-1} \sim \alpha\omega_c(v/c)^2$ , where  $\alpha$  is the fine structure  
 276 constant,  $c$  speed of light in vacuum and the character-  
 277 istic  $\omega_c$  cyclotron frequency ( $\tau_{\text{sp}} \approx 10^{-6}$  s in the THz  
 278 range for  $v = 10^6$  m/s). Hence, there still exist other  
 279 (non-radiative) channels which dominate the recombi-  
 280 nation, such as electron-phonon interaction giving rise to  
 281 emission of phonons.

282 The observed slowing-down in the relaxation dynamics  
 283 of electrons induced by the magnetic field, with the the  
 284 overall lifetime of photo-excited electrons in the nanosec-  
 285 ond range, call for cyclotron emission experiments. We  
 286 have performed such experiments in the THz spectral  
 287 range, which is the most relevant one for applications of  
 288 the future Landau level laser technology. To generate  
 289 cyclotron emission, the sample was placed in a super-  
 290 conducting coil at liquid helium temperature and electri-

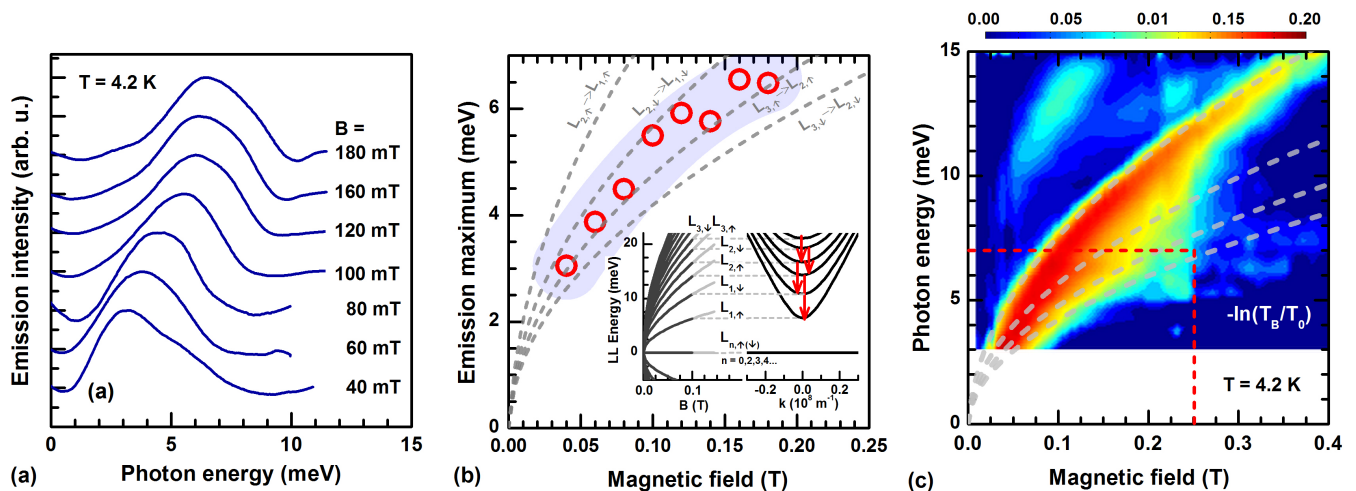


FIG. 4. **Cyclotron-emission and absorption of 3D massless Kane electrons.** (a) Cyclotron emission spectra measured on gapless HgCdTe sample kept in the liquid helium at selected values of the magnetic field. (b) Experimentally deduced maxima of emission compared with theoretically expected cyclotron modes (dashed lines), see the text. The grey area correspond to the error bar of cyclotron emission maxima. The LL spectrum with schematically depicted emission lines (by vertical arrows) is shown in the inset. (c) The false-color map of magneto-absorbance, primarily due to cyclotron resonance absorption, reprinted from Ref. 31. The dashed lines show the theoretically expected positions of cyclotron modes, the same ones as in (b). The red dashed lines shows the range of magnetic fields and photon energies in which cyclotron emission was explored.

291 cally pumped, using ms-long current pulses, see Meth- 323  
 292 ods section. The emitted radiation was analyzed using 324  
 293 a photoconductive InSb detector, with a spectrally 325  
 294 narrow (cyclotron-resonance-like) response, tunable by a 326  
 295 specially dedicated coil. The collected cyclotron emission 327  
 296 spectra are plotted in Fig. 4a for selected values of the 328  
 297 magnetic field applied to the sample. 329

298 A brief inspection of the emission spectra leads us to 332  
 299 a conclusion that they feature a single emission band. 333  
 300 Its position in the spectrum is tunable in the THz range 334  
 301 by a relatively low magnetic field (tens of millitesla) and 335  
 302 it roughly follows a  $\sqrt{B}$  dependence, which is typical of 336  
 303 massless electrons (Fig. 4b). This also agrees well with 337  
 304 results of cyclotron absorption experiments performed on 338  
 305 the same sample, see Fig. 4c and Ref. 31. However, a 339  
 306 closer look at the lineshape suggests that several emis- 340  
 307 sion modes actually contribute. Theoretically, one indeed 341  
 308 expects several cyclotron emission modes in the interval 342  
 309 given by the linewidth (FWHM  $\sim 4$  meV). In Fig. 4b, 343  
 310 the dashed lines show the positions of cyclotron emis- 344  
 311 sion modes with the final states of electrons in the four 345  
 312 lowest lying conduction-band LLs:  $E_{N+1,\uparrow(\downarrow)}^K \rightarrow E_{N,\uparrow(\downarrow)}^K$  346  
 313 for  $N = 1$  and 2. It is thus the spacing of these cyclo- 347  
 314 tron modes, together with primarily elastic scattering 348  
 315 processes, which is responsible for the observed width of 349  
 316 the emission band. The mutual intensities of individual 350  
 317 modes then determine the position of the maximum of 351  
 318 the emission band. At higher  $B$ , the relative weight of 352  
 319 modes from higher LLs increases, which reflects the dis- 353  
 320 tribution of electrons among LLs established by electrical 354  
 321 pumping and which leads to a slowing-down of the  $\sqrt{B}$  355  
 322 dependence.

323 Even though the cyclotron emission observed in the 324  
 325 used configuration is primarily due to spontaneous re- 326  
 327 combination, it is worth to discuss conditions required 328  
 329 to obtain stimulated emission and gain. To achieve 329  
 330 the light amplification comparable to, *e.g.*, quantum 330  
 331 cascade lasers<sup>38</sup>, the gain coefficient has to approach 331  
 332  $g = \Delta n \cdot \sigma \sim 10$  cm<sup>-1</sup>, where  $\Delta n$  stands for the popu- 332  
 333 lation inversion and  $\sigma = \lambda^2 / (2\pi) \cdot (\tau_{\text{tot}} / \tau_{\text{sp}})$  is the stimu- 333  
 334 lated emission cross-section<sup>39</sup>. The typical spontaneous 334  
 335 cyclotron emission lifetime of massless electrons in the 335  
 336 THz range reaches  $\tau_{\text{sp}} \sim 1$   $\mu$ s and the total lifetime, 336  
 337 which dominantly reflects elastic scattering, may be esti- 337  
 338 mated (its lower limit) from the linewidth of the emission 338  
 339 line:  $\tau_{\text{tot}} \sim 1$  ps. Taking the characteristic wave length of 339  
 340  $\lambda = 300$   $\mu$ m, we obtain the cross-section  $\sigma \sim 10^{-10}$  cm<sup>-2</sup>. 340  
 341 This implies the necessity to achieve the population in- 341  
 342 version  $\Delta n > 10^{11}$  cm<sup>-3</sup>. Our simple estimate, see Sup- 342  
 343 plementary materials<sup>40</sup>, indicates that such a popula- 343  
 344 tion inversion should be achievable at least in the pulsed 344  
 345 mode.

343 To conclude, we have demonstrated, for the first time, 343  
 344 cyclotron emission of massless electrons. This emission 344  
 345 was observed in gapless HgCdTe – a system hosting 345  
 346 3D massless Kane electrons. The existence of sizeable 346  
 347 cyclotron emission is directly related to their particu- 347  
 348 lar Landau level spectrum, which comprises only non- 348  
 349 equidistantly spaced levels. The systems hosting massless 349  
 350 Kane electrons are thus promising candidates for an ac- 350  
 351 tive medium of a Landau level laser, which would, in this 351  
 352 particular case, operate in the THz and infrared spectral 352  
 353 ranges and would be widely tunable by very low magnetic 353  
 354 fields. 354

## 355 Methods

356 *Sample growth.* The sample was grown using standard  
357 molecular-beam epitaxy on a (013)-oriented semi-insulating  
358 GaAs substrate. The growth sequence started with ZnTe and  
359 CdTe transition regions, followed by the MCT epilayer with  
360 gradually changing cadmium content  $x$ . The prepared MCT  
361 layer contains a region with  $x \approx 0.17$  of thickness  $d \approx 3.2 \mu\text{m}$ .  
362 For more details about the explored sample see Ref. 31.

363 *Pump-probe spectroscopy.* The free-electron laser FELBE  
364 provided frequency-tunable Fourier-limited radiation pulses.  
365 In the experiments described in this paper, photon energies  
366 of  $\hbar\omega = 61$  and  $78$  meV were chosen. The pulse duration was  
367 about  $3$  ps, the repetition rate was  $13$  MHz. The pulses were  
368 split into pump and probe pulses by a pellicle beam splitter.  
369 The polarizations of pump and probe beams were controlled  
370 independently. Frequency-tunable quarter-wave plates (from  
371 Alphalas GmbH) were used for the generation of circularly  
372 polarized radiation. Both the pump and probe beam were  
373 focused on the sample in the magnet cryostat by an off-axis  
374 parabolic mirror (effective focal length:  $178$  mm). The spot  
375 size on the sample was  $\sim 0.5$  mm (FWHM). The pump fluence  
376 was  $\sim 0.5 \mu\text{J}\cdot\text{cm}^{-2}$ , the fluence of the probe beam was about  
377  $10\%$  of the pump fluence. The time delay between pump and  
378 probe pulses was varied using a mechanical delay stage.

379 *Emission measurements.* To measure radiation emitted  
380 due to inter-LL recombination of electrons, the radiation was  
381 guided, using a copper light pipe, to a InSb photoconductive  
382 spatially separated from the coil inside which the sample was  
383 placed. The used detector has narrow-band ( $\sim 60$  GHz) and  
384 field-tunable response due to cyclotron resonance absorption.  
385 This tunability is ensured by a specially dedicated supercon-  
386 ducting coil and allows us to analyze the radiation in the  
387 spectral range of  $0.4$ - $2.5$  THz. All emission experiments oper-  
388 ate in a pulsed mode (using current pulses for pumping), with

389 the pulse duration of  $7$  ms and with the peak-to-peak value  
390 of electric field up to  $12$  V/cm. The duty circle was tuned in  
391 such a way that the average power consumption of emitter did  
392 not exceed  $13$  mW (to avoid sample heating). The signal on  
393 the InSb detector was collected using a conventional lock-in  
394 technique.

## 395 Additional information

396 The authors declare no competing financial interests. Cor-  
397 respondence and requests for materials should be addressed  
398 to M.O.

## 399 Acknowledgements

400 The authors acknowledge helpful discussions with D. M.  
401 Basko and R. J. Nicholas. This work was supported by ANR  
402 DIRAC3D project. The research was also partially supported  
403 by the Occitanie region and MIPS department of Montpellier  
404 University via the Terahertz Occitanie platform, and by the  
405 Foundation for Polish Science through the TEAM and IRA  
406 Programs financed by EU within SG OP Program. Part of  
407 this work has been supported by the project CALIPSO under  
408 the EC Contract No. 312284.

## 409 Author contributions

410 The experiment was proposed by M.O. and M.P. The sam-  
411 ple was grown by N.N.M. and S.A.D. Time-resolved and cw  
412 magneto-optical experiments were carried out by M.O., M.M.,  
413 S.W., C.F. and M.H. The cyclotron emission experiments  
414 were performed by D.B., C.C., F.T. and W.K. All coau-  
415 thors discussed the experimental data and interpretation of  
416 results. M.O. and M.P. wrote the manuscript, all coauthors  
417 commented on it.

## 418 Data and code availability

419 The data that support the findings of this study as well as  
420 the code for modelling of cyclotron mode energies are available  
421 from the corresponding author on reasonable request.

422 \* milan.orlda@lncmi.cnrs.fr

423 M. L. Cohen, "Cyclotron resonance and quasiparticles," *AIP*  
424 *Conference Proceedings* **772**, 3–6 (2005).

425 B. Lax, "Cyclotron resonance and impurity levels in  
426 semiconductors," in *Proceedings of the International*  
427 *Symposium on Quantum Electronics*, edited by C. H.

428 Townes (Columbia Univ. Press, New York, 1960) p. 428.

429 E. Gornik, "Landau emission in semiconductor," in *Narrow*  
430 *Gap Semiconductors. Physics and Applications. Lecture*  
431 *Notes in Physics*, Vol. 133, edited by W. Zawadzki  
432 (Springer, Berlin, 1980).

433 E. Gornik, "Proceedings of the 4th general conference of the  
434 condensed matter division of the eps far infrared light  
435 emitters and detectors," *Physica B+C* **127**, 95 – 103 (1984).

436 W. Knap, D. Dur, A. Raymond, C. Meny, J. Leotin,  
437 S. Huant, and B. Etienne, "A far-infrared spectrometer  
438 based on cyclotron resonance emission sources," *Review of*  
439 *Scientific Instruments* **63**, 3293–3297 (1992).

440 T. H. Maiman, "Stimulated optical radiation in ruby,"  
441 *Nature* **187**, 493–494 (1960).

442 P. A. Wolff, "Proposal for a cyclotron resonance maser in  
443 insb," *Physica Physique Fizika* **1**, 147–157 (1964).

444 P. A. Wolff, "Cyclotron resonance laser," patent US3265977

445 (1966).

446 H. Aoki, "Novel Landau level laser in the quantum hall  
447 regime," *Applied Physics Letters* **48**, 559–560 (1986).

448 T. Morimoto, Y. Hatsugai, and H. Aoki, "Cyclotron  
449 radiation and emission in graphene," *Phys. Rev. B* **78**,  
450 073406 (2008).

451 C Sirtori, "Applied physics - bridge for the terahertz gap,"  
452 *Nature* **417**, 132–133 (2002).

453 M. Tonouchi, "Cutting-edge terahertz technology," *Nature*  
454 *Photonics* **1**, 97–105 (2007).

455 E. Gornik, T. Y. Chang, T. J. Bridges, V. T. Nguyen, J. D.  
456 McGee, and W. Müller, "Landau-Level-Electron lifetimes in  
457  $n$ -InSb," *Phys. Rev. Lett.* **40**, 1151–1154 (1978).

458 M. Potemski, R. Stepniowski, J. C. Maan, G. Martinez,  
459 P. Wyder, and B. Etienne, "Auger recombination within  
460 Landau levels in a two-dimensional electron gas," *Phys. Rev.*  
461 *Lett.* **66**, 2239–2242 (1991).

462 E. Tsitsishvili and Y. Levinson, "Auger scattering between  
463 Landau levels in a two-dimensional electron gas," *Phys. Rev.*  
464 *B* **56**, 6921–6930 (1997).

465 Jürgen Schneider, "Stimulated emission of radiation by  
466 relativistic electrons in a magnetic field," *Phys. Rev. Lett.* **2**,  
467 504–505 (1959).

- <sup>17</sup><sub>468</sub> K. Unterrainer, C. Kremser, E. Gornik, C. R. Pidgeon,  
<sup>469</sup> Yu. L. Ivanov, and E. E. Haller, “Tunable  
<sup>470</sup> cyclotron-resonance laser in germanium,” *Phys. Rev. Lett.*  
<sup>471</sup> **64**, 2277–2280 (1990).
- <sup>18</sup><sub>472</sub> Stephane Blaser, Michel Rochat, Mattias Beck, Daniel  
<sup>473</sup> Hofstetter, and Jerom Faist, “Terahertz intersubband  
<sup>474</sup> emission in strong magnetic fields,” *Applied Physics Letters*  
<sup>475</sup> **81**, 67–69 (2002).
- <sup>19</sup><sub>476</sub> François-Régis Jasnot, Louis-Anne de Vaultier, Yves  
<sup>477</sup> Guldner, Gérald Bastard, Angela Vasanelli, Christophe  
<sup>478</sup> Manquest, Carlo Sirtori, Mattias Beck, and Jérôme Faist,  
<sup>479</sup> “Direct surface cyclotron resonance terahertz emission from  
<sup>480</sup> a quantum cascade structure,” *Applied Physics Letters* **100**,  
<sup>481</sup> 102103 (2012).
- <sup>20</sup><sub>482</sub> T. Morimoto, Y. Hatsugai, and H. Aoki, “Cyclotron  
<sup>483</sup> radiation and emission in graphene – a possibility of  
<sup>484</sup> Landau-level laser,” *Journal of Physics: Conference Series*  
<sup>485</sup> **150**, 022059 (2009).
- <sup>21</sup><sub>486</sub> F. Wendler and E. Malic, “Towards a tunable  
<sup>487</sup> graphene-based Landau level laser in the terahertz regime,”  
<sup>488</sup> *Scientific Reports* **5**, 12646 (2015).
- <sup>22</sup><sub>489</sub> Y. Wang, M. Tokman, and A. Belyanin, “Continuous-wave  
<sup>490</sup> lasing between Landau levels in graphene,” *Phys. Rev. A*  
<sup>491</sup> **91**, 033821 (2015).
- <sup>23</sup><sub>492</sub> S. Brem, F. Wendler, and E. Malic, “Microscopic modeling  
<sup>493</sup> of tunable graphene-based terahertz Landau-level lasers,”  
<sup>494</sup> *Phys. Rev. B* **96**, 045427 (2017).
- <sup>24</sup><sub>495</sub> N. Cole and T. M. Antonsen, “Electron cyclotron resonance  
<sup>496</sup> gain in the presence of collisions,” *IEEE Transactions on*  
<sup>497</sup> *Plasma Science* **45**, 2945–2954 (2017).
- <sup>25</sup><sub>498</sub> S. Brem, F. Wendler, S. Winnerl, and E. Malic,  
<sup>499</sup> “Electrically pumped graphene-based Landau-level laser,”  
<sup>500</sup> *Phys. Rev. Materials* **2**, 034002 (2018).
- <sup>26</sup><sub>501</sub> P. Plochocka, P. Kossacki, A. Golnik, T. Kazimierzuk,  
<sup>502</sup> C. Berger, W. A. de Heer, and M. Potemski, “Slowing  
<sup>503</sup> hot-carrier relaxation in graphene using a magnetic field,”  
<sup>504</sup> *Phys. Rev. B* **80**, 245415 (2009).
- <sup>27</sup><sub>505</sub> M. Mittendorff, F. Wendler, E. Malic, A. Knorr, M. Orlita,  
<sup>506</sup> M. Potemski, C. Berger, W. A. de Heer, H. Schneider,  
<sup>507</sup> M. Helm, and S. Winnerl, “Carrier dynamics in  
<sup>508</sup> Landau-quantized graphene featuring strong Auger  
<sup>509</sup> scattering,” *Nature Physics* **11**, 75 (2015).
- <sup>28</sup><sub>510</sub> Jacob C. König-Otto, Yongrui Wang, Alexey Belyanin,  
<sup>511</sup> Claire Berger, Walter A. de Heer, Milan Orlita, Alexej  
<sup>512</sup> Pashkin, Harald Schneider, Manfred Helm, and Stephan  
<sup>513</sup> Winnerl, “Four-wave mixing in Landau-Quantized  
<sup>514</sup> graphene,” *Nano Letters* **17**, 2184–2188 (2017).
- <sup>29</sup><sub>515</sub> E. O. Kane, “Band structure of indium antimonide,” *J.*  
<sup>516</sup> *Phys. Chem. Solids* **1**, 249 – 261 (1957).
- <sup>30</sup><sub>517</sub> P. Kacman and W. Zawadzki, “Spin magnetic moment and  
<sup>518</sup> spin resonance of conduction electrons in  $\alpha$ -Sn-type  
<sup>519</sup> semiconductors,” *phys. stat. sol. (b)* **47**, 629–642 (1971).
- <sup>31</sup><sub>520</sub> M. Orlita, D. M. Basko, M. S. Zholudev, F. Teppe,  
<sup>521</sup> W. Knap, V. I. Gavrilenko, N. N. Mikhailov, S. A.  
<sup>522</sup> Dvoretiskii, P. Neugebauer, C. Faugeras, A.-L. Barra,  
<sup>523</sup> G. Martinez, and M. Potemski, “Observation of  
<sup>524</sup> three-dimensional massless Kane fermions in a zinc-blende  
<sup>525</sup> crystal,” *Nature Physics* **10**, 233 (2014).
- <sup>32</sup><sub>526</sub> F. Teppe, M. Marcinkiewicz, S.S. Krishtopenko,  
<sup>527</sup> S. Ruffenach, C. Consejo, A.M. Kadykov, W. Desrat,  
<sup>528</sup> D. But, W. Knap, J. Ludwig, S. Moon, D. Smirnov,  
<sup>529</sup> M. Orlita, Z. Jiang, S.V. Morozov, V.I. Gavrilenko, N.N.  
<sup>530</sup> Mikhailov, and S.A. Dvoretiskii, “Temperature-driven  
<sup>531</sup> massless Kane fermions in HgCdTe crystals: verification of  
<sup>532</sup> universal velocity and rest-mass description,” *Nature*  
<sup>533</sup> *Communications* **7**, 12576 (2016).
- <sup>33</sup><sub>534</sub> V. B. Berestetskii, E. M. Lifshitz, and L. P. Pitaevskii,  
<sup>535</sup> *Relativistic Quantum Theory*, A Course of Theoretical  
<sup>536</sup> Physics, Vol. 4, part 1 (Pergamon, 1971).
- <sup>34</sup><sub>537</sub> M.H. Weiler, “Chapter 3 magneto-optical properties of  
<sup>538</sup>  $\text{Hg}_{1-x}\text{Cd}_x\text{Te}$  alloys,” in *Defects, (HgCd)Se, (HgCd)Te*,  
<sup>539</sup> Semiconductors and Semimetals, Vol. 16, edited by R.K.  
<sup>540</sup> Willardson and Albert C. Beer (Elsevier, 1981) pp. 119 –  
<sup>541</sup> 191.
- <sup>35</sup><sub>542</sub> S. Winnerl, M. Orlita, P. Plochocka, P. Kossacki,  
<sup>543</sup> M. Potemski, T. Winzer, E. Malic, A. Knorr, M. Sprinkle,  
<sup>544</sup> C. Berger, W. A. de Heer, H. Schneider, and M. Helm,  
<sup>545</sup> “Carrier relaxation in epitaxial graphene photoexcited near  
<sup>546</sup> the Dirac point,” *Physical Review Letters* **107**, 237401  
<sup>547</sup> (2011).
- <sup>36</sup><sub>548</sub> E. Gornik, “Far infrared light emitters and detectors,”  
<sup>549</sup> *Physica B+C* **127**, 95 – 103 (1984), proceedings of the 4th  
<sup>550</sup> General Conference of the Condensed Matter Division of the  
<sup>551</sup> EPS.
- <sup>37</sup><sub>552</sub> M. O. Goerbig, “Electronic properties of graphene in a  
<sup>553</sup> strong magnetic field,” *Rev. Mod. Phys.* **83**, 1193–1243  
<sup>554</sup> (2011).
- <sup>38</sup><sub>555</sub> Sirtori, C., “Gaas quantum cascade lasers: Fundamentals  
<sup>556</sup> and performance,” *Collection de la Société Française*  
<sup>557</sup> *d’Optique* **7**, 03 (2002).
- <sup>39</sup><sub>558</sub> Bahaa E A Saleh and Malvin Carl Teich, *Fundamentals of*  
<sup>559</sup> *photonics; 2nd ed.*, Wiley series in pure and applied optics  
<sup>560</sup> (Wiley, New York, NY, 2007).
- <sup>40</sup><sub>561</sub> See Supplementary materials.